Available online at www.sciencedirect.com
SCIENCE DIRECT
Journal of Power Sources 156 (2006) 33–38
JOURNAL OF POWER SOURCES
www.elsevier.com/locate/jpowsour

Short communication

Composition and porosity graded $La_{2-x}NiO_{4+\delta}$ ($x \geq 0$) interlayers for SOFC: Control of the microstructure via a sol–gel process

M.L. Fontaine *, C. Laberty-Robert, F. Ansart, P. Tailhades

CIRIMAT/LCMIE, Paul Sabatier University, 31062 Toulouse, France

Available online 2 November 2005

Abstract

We have developed composition and porosity graded $La_{2-x}NiO_{4+\delta}$ ($x \geq 0$) cathode interlayers for low-temperature solid oxide fuel cell that exhibit good adhesion with the electrolyte, controlled porosity and grain size and good electrochemical behaviour. $La_{2-x}NiO_{4+\delta}$ ($x \geq 0$) monolayers are elaborated from a derived sol–gel method using nitrate salts, acetylacetone and hexamethylenetetramine in acetic acid. As a function of the organic concentration and the molar ratio of lanthanum to nickel, these layers present platelets or spherical shape grains with a size distribution ranging from 50 to 200 nm, as verified by SEM-FEG. On the basis of this processing protocol, we prepared porosity and composition graded lanthanum nickelates interlayers with effective control of the pore distribution, the nanocrystalline phase, the thickness and the subsequent electrochemical properties.

Keywords: Cathodic interlayers; Microstructure; SOFC; Sol–gel

1. Introduction

One of the most important goals in SOFC research is the reduction of the working temperature from 900–1000 °C to about 700 °C for future applications. This would allow metallic interconnects work reliable [1], use of SOFCs in smaller power plant applications that require on/off cycling [2], and direct operation with hydrocarbon fuels by reducing the coking rates [3]. However, at intermediate temperature, one of the main limiting factors is the high polarization resistance of usual cathode materials, such as $La_{1-x}Sr_xMnO_{3+\delta}$ (LSM) oxides, which limits SOFC power densities [4]. Consequently, much attention has recently been focused on improving the cathodic performance by both using mixed ionic and electronic conductor materials and improving the microstructural design at the cathode/electrolyte interface. Recent studies on mixed conductors indicated that the Ruddlesden–Popper phases with the K_2NiF_4-type structure have promising properties at intermediate operating temperatures [5] due to their high ionic conduction and their high electrocatalytic activity, which were correlated to additional oxygen on interstitial site and presence of cations with different oxidation states. As large variability in performance can occur depending on the geometric design of the fuel cell and both the microstructural and the compositional parameters of the electrodes, development of new designs has been extensively investigated through both experimental and modeling approaches [6–9]. For example, it indicated that cathodic performance can be improved by using a thin layer with flat surface and small grains diameter at the cathode/electrolyte interface, covered by a thicker and porous layer with larger grains. This duplex microstructure design increases the reaction zone and ensures the current collection by the additional porous layer. Promising results are also obtained for microstructural electrolyte design consisting in the YSZ substrates covered by YSZ particles [8]. Indeed, this configuration allows an enlargement of the electrochemical active surface area at the cathode/electrolyte interface.

Extending these several approaches, we focused on the synthesis of a thin and functionally cathodic interlayer with high specific surface area that will be covered by a thicker porous layer. To achieve this goal, sol–gel process is very attractive as it provides an easy control of both microstructure and composition of electrode materials, allows low-temperature processing and strong interaction between the electrode and the electrolyte. Our processing protocols also allow the control of the pore-solid architecture and then, an improvement of the subsequent electrochemical properties of $La_2NiO_{4+\delta}$ electrodes [10].

In this paper, we report an extension of our previous approach in view of synthesizing the $Ln_{2-x}NiO_{4+\delta}$ ($x \geq 0$) thin graded

* Corresponding author. Tel.: +47 40 00 37 30; fax: +47 98 24 34 99.
E-mail address: marie-laure.fontaine@sintef.no (M.L. Fontaine).

0378-7753/$ – see front matter © 2005 Elsevier B.V. All rights reserved.
doi:10.1016/j.jpowsour.2005.08.016

porosity and composition cathodic interlayers. These layers are elaborated using the dip-coating method with the control of the organic concentration, the ratio of transition metals, the number of coats and the withdrawal speed. The processing protocol and the electrochemical performance of the duplex microstructure electrodes will be presented in a forthcoming paper.

2. Experimental details

2.1. Preparation of porosity and functionally graded electrodes

$La_{2-x}NiO_{4+\delta}$ ($x \geq 0$) thin films were prepared using a modified citrate route [11]. A stoichiometric mixture of the relevant nitrates was dissolved in a small amount of water. This solution was combined to an organic solution of hexamethylenetetramine and acetyl acetone added in a molar ratio (1:1), in acetic acid. Controlled organic compounds content is critical to obtain the pure phase [12]. Thus, a range of molar ratio of complexing agent to nitrate species (called R) has been defined. Pure Ruddlesden–Popper phase is obtained for R ratio ranging from 2 to 3. Above $R = 3$, the strong heat released during the organics pyrolysis leads to the formation of a mixture of oxides (La_2O_3, $La_2NiO_{4+\delta}$, $La_3Ni_2O_7$) [12]. Same mixture is also obtained for $R < 2$, due to a heterogeneous cationic chelation [13]. The resulting solution was then stirred and heated at 70 °C until sols with a viscosity of 45 mPa s were obtained.

Commercial YSZ pellets (LEPMI, Grenoble, France) were used as substrates. In order to have a strong interaction between YSZ and $La_{2-x}NiO_{4+\delta}$ ($x \geq 0$) cathodic interlayers, the substrates were first polished up to a roughness of 20 nm. Lanthanum nickelates layers were then, dip-coated on both sides of the pellets in order to prepare symmetrical half cell.

For monolayers synthesis, the symmetrical cells were heated slowly up to 700 °C with a heating rate of 50 °C h^{-1} to prevent cracks during the organics decomposition. They were then annealed at 1000 °C for 2 h with a heating rate of 100 °C h^{-1} [14].

Previous studies showed that the A-site non-stoichiometry strongly affects the oxygen non-stoichiometry and then, both ionic and electronic conductivities of the oxides [14]. Thus, porosity and composition graded multilayers were prepared from the dip-coat of sols synthesized with various R ($R = 2$ and 3) and various molar ratio of lanthanum to nickel r ($r = 2$, 1.98). To confirm the composition grades, atomic absorption spectroscopy and X-ray diffraction analyses were performed on powders synthesized from each as-prepared sol annealed in air at 1000 °C.

In order to increase the films thickness, several coats were deposited onto YSZ substrates with different withdrawal speeds ranging from 1 to 4 cm min^{-1}. The heat treatment used between each coat strongly affects the film microstructure (particle size and porosity) and may be used to modify the physical properties of the films [15]. For this study, the intermediate heat treatment was 700 °C; this temperature corresponds to both the burnout of the organic compounds and the formation of small crystallites in the film. The symmetrical half cell was then fired at 1000 °C to ensure that the phase was well-formed with controlled porosity.

2.2. Viscosity

The sol viscosity was measured with a rotating-spindle viscosimeter (Lamy Tve-05). Sets of measurements were taken at all rotational speeds.

2.3. X-ray diffraction analysis

Thin films structural investigations were carried out with a Seifert XRD 3003 diffractometer using the Cu Kα radiation (Cu Kα1 = 1.5405, Cu Kα2 = 1.5443).

2.4. Microstructural characterizations

Thin films microstructure was studied by scanning electron microscopy coupled with a field emission gun SEM-FEG (JEOL-JSM-6700F). Both cathode/electrolyte interfaces and cathode surfaces were observed. Considering the different parameters used to prepare these films, the cathodic interlayers will be referenced in this paper as following: C[(R,r)–···–(R,r)] where each bracket represents one coat listed from the top of the YSZ pellet. R corresponds to the molar ratio of complexing agent to nitrate species and r is the molar ratio of lanthanum to nickel. The thin films thickness was also evaluated with an optical profilometer Zygometer (3D "ZYGO").

3. Results

3.1. Influence of the sol synthesis parameters on the films microstructure

Grazing angle X-ray diffraction patterns of $La_{2-x}NiO_{4+\delta}$ ($x \geq 0$) thin films are obtained for composition and porosity graded electrodes calcined at 1000 °C for 2 h. Fig. 1 shows the pattern obtained for $La_2NiO_{4+\delta}$ multilayers prepared with $R = 3$ and three coats, using a grazing angle of 1°.

Under these conditions, the peaks corresponding to the YSZ substrate can be observed indicating that the X-ray beam goes through the $La_2NiO_{4+\delta}$ film. Only $La_2NiO_{4+\delta}$ phase peaks are observed.

In Fig. 2, is reported the influence of the organic compounds content ($R = 2$ and 3) and the final annealed temperature (700

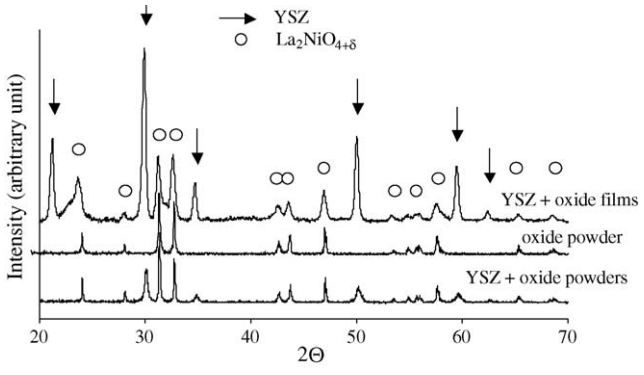

Fig. 1. Grazing angle X-ray diffraction pattern of C[(3,2)] $La_2NiO_{4+\delta}$ film, deposited on YSZ substrate and annealed at 1000 °C.

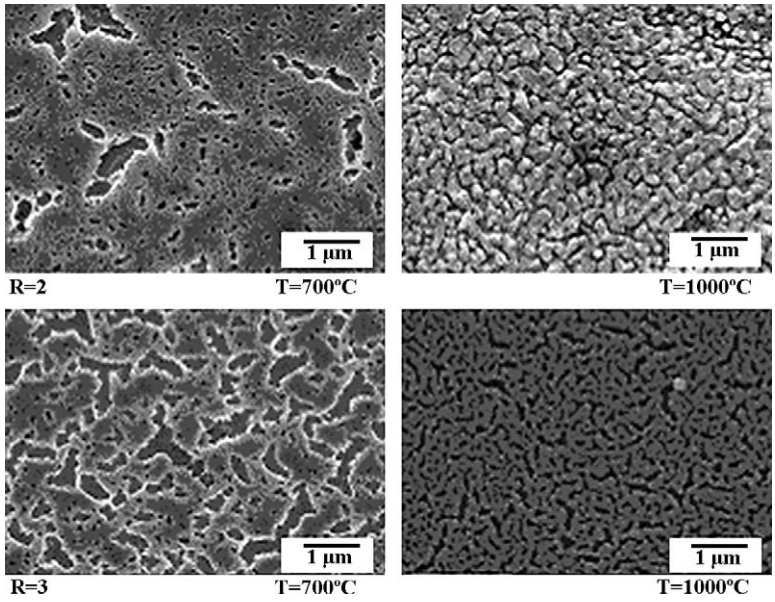

Fig. 2. SEM micrographs of $La_2NiO_{4+\delta}$ monolayers annealed at 700 and 1000 °C.

and 1000 °C) on the microstructure of $La_2NiO_{4+\delta}$ monolayers. The microstructural parameters of these films are reported in Table 1.

Fig. 2 shows that the films microstructure strongly depends on both the annealing temperature and the *R* ratio. In our process, a heat treatment is required to get crystallized oxides. This stage affects the films microstructure and, in particular, the porosity.

For a heating temperature of 700 °C, the small grains have a spherical shape (3D growth) and are randomly oriented, whatever the *R* ratio used. Moreover, layers are characterized by a high porosity with a large pore size.

In contrast, for a heating temperature of 1000 °C, the grains present specific texture, shape and size depending on the *R* ratio. For $R = 2$, a 2D growth of the particles has occurred, leading to the formation of elongated grains or platelets along the substrate surface so that the films are characterized by a near-uniform fibre texture. A bimodal distribution of the grain sizes is also observed. For $R = 3$, the films remain randomly oriented. A monomodal grain sizes distribution developed and the grains shape remains spherical with a grain size distribution lower than 50 nm. Thus, the comparison of the films microstructure shows that the lowest the *R* ratio, the denser the films.

To increase the film thickness, multilayers were synthesized with two coats deposited onto the YSZ substrate, using either the same *R* or two different *R* ($R = 2$ and 3). Fig. 3 shows the surface of these layers annealed in air at 1000 °C. As example, a cross-section of the C[(3,2)–(2,2)] porosity graded layer can also be observed in this figure. The microstructural parameters of these electrodes are reported in Table 2.

Homogeneous and crack-free films are obtained, whatever the used conditions. $La_2NiO_{4+\delta}$ bilayers prepared either with $R = 2$ or 3 have a well-defined grain structure depending on the organic compounds content. Indeed, the shape of the grain size distribution does not change with the films thickness. For $R = 3$, the grains size distribution remains monomodal, whereas a bimodal distribution is still observed for electrodes synthesized with $R = 2$. The same behaviour has also been observed for layers made with three and four coats.

The mean grains size for C[(3,2)–(3,2)] interlayer is about 2.5 times lower than the one obtained for C[(2,2)–(2,2)]. As there is a little change in the films thickness, this explains the variation of the porosity (Table 2). Porosity graded interlayers present a similar pore-solid architecture than the one observed for C[(2,2)–(2,2)]. However, the particle size is higher, causing a densification of the films (Table 2).

Similar microstructure is also observed for composition graded layers as shown in Figs. 4 and 5. Their microstructural parameters are reported in Table 3. The main difference for composition graded films is on the mean grains size. As the cationic concentration decreases with *r*, this may be explained the variation in grain size. The smaller the cationic concentration in the

Table 1
Microstructural parameters of $La_2NiO_{4+\delta}$ monolayers annealed at 1000 °C with $R = 2$ and 3

Dwelling temperature	*R*	Thickness (±10 nm)	Mean grain size (±10 nm)	Porosity (±3%)
1000 °C	2	75	50–110	30
	3	90	35	37
700 °C	2	120	35	37
	3	135	<10	53

Table 2
Microstructural parameters of bilayers annealed at 1000 °C with various *R* ratios

Interlayers	Thickness (±10 nm)	Mean grain size (±10 nm)	Pore size (±10 nm)	*P* (±3%)
C[(2,2)–(2,2)]	220	135	100–1000	23
C[(3,2)–(3,2)]	250	55	100–250	34
C[(2,2)–(3,2)]	230	200	100–250	18
C[(3,2)–(2,2)]	230	175	100–250	20

P: porosity.

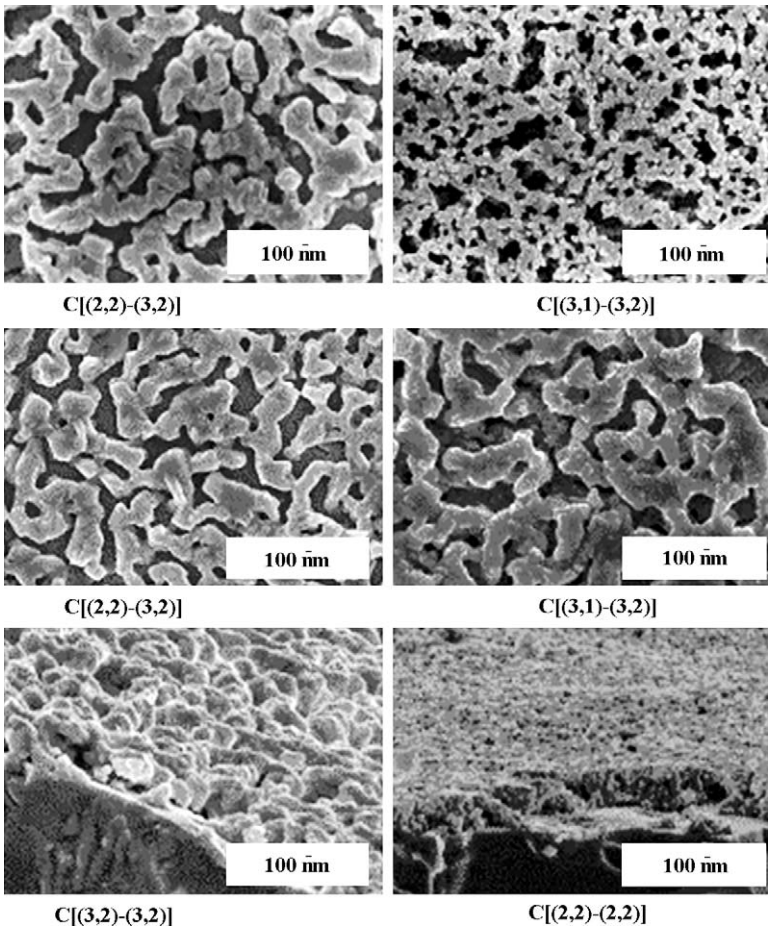

Fig. 3. SEM-FEG micrographs of $La_2NiO_{4+\delta}$ bilayers: C[(2,2)–(2,2)], C[(3,2)–(3,2)], C[(2,2)–(3,2)], C[(3,2)–(2,2)]; cross-section of interlayers C[(2,2)–(2,2)] and C[(3,2)–(3,2)].

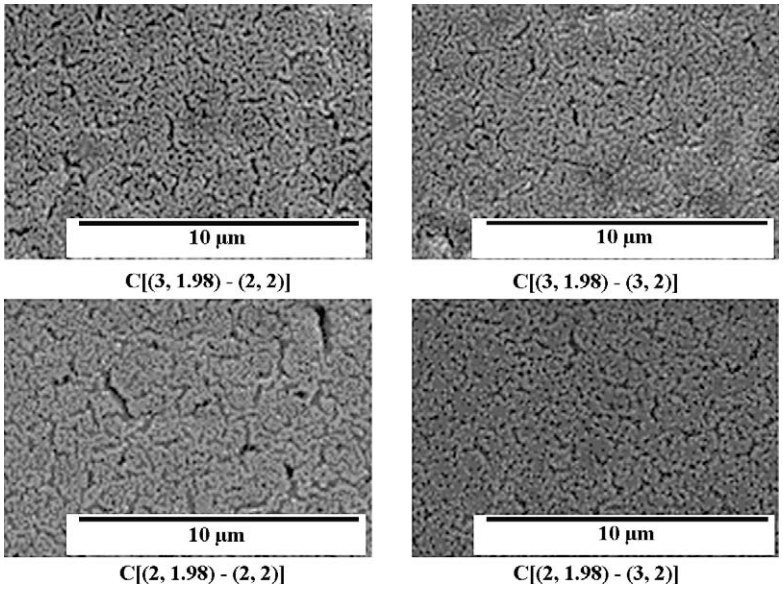

Fig. 4. SEM micrographs of interlayers with gradual porosity and compositions.

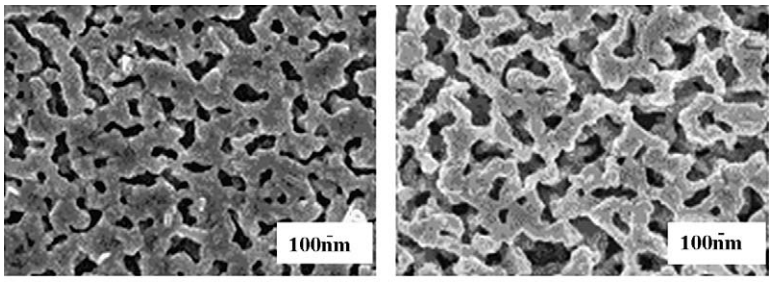

Fig. 5. SEM-FEG micrographs of interlayers with gradual porosity and compositions.

Table 3
Microstructural parameters of bilayers annealed at 1000 °C with various *R* and *r* ratios

Interlayers	Thickness (±10 nm)	Mean grain size (±10 nm)	Pore size (±10 nm)	*P* (±3%)
C[(2,1.98)–(3,2)]	180	85	100–250	24
C[(2,1.98)–(2,2)]	200	75	100–300	27
C[(3,1.98)–(3,2)]	220	50	100–250	30
C[(3,1.98)–(2,2)]	210	89	100–300	30

P: porosity.

sol, the smaller quantity of matter deposited, the slower grains growth and the worst percolation between grains.

3.2. Influence of the physical parameters on the films microstructure

In order to elaborate homogeneous and crack-free films with the highest thickness, several coats were deposited onto the YSZ substrates with different withdrawal speeds ranging from 1 to 4 cm min^{-1}. In Fig. 5 is reported the evolution of the thickness of $La_2NiO_{4+\delta}$ films as a function of the number of coats, the withdrawal speed and the *R* ratio.

As shown in Fig. 6, the higher both the number of coats and the withdrawal speed, the higher the electrode thickness, whatever the *R* ratio. However, a limit in the withdrawal speed is defined as crack films were obtained for withdrawal speeds higher than 4 cm min^{-1}. Previous thermal analyses showed that the decomposition of the polymeric sol is strongly exothermic, especially during the burnout of the organic compounds from 300 to 600 °C [14].

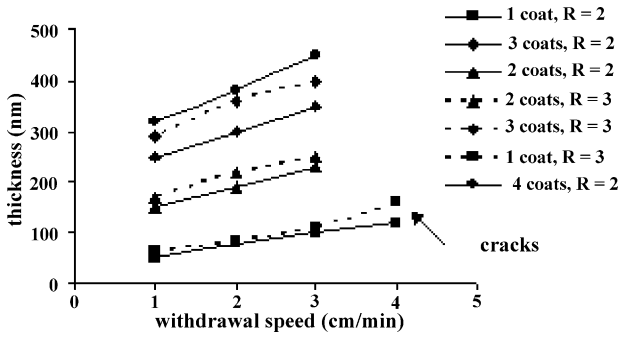

Fig. 6. Evolution of the thickness of $La_2NiO_{4+\delta}$ multilayers prepared with *R* = 2 and 3 as a function of the withdrawal speed and the number of coats.

Accordingly, the increase in the withdrawal speed conduces to an increase in the precursor layer thickness, leading to the occurrence of a very large amount of shrinkages in the film during the heating step. This will cause film cracking when the withdrawal speed is too high. Thus, a balance between withdrawal speed and thickness is necessary in order to obtain crack-free films. Cracked films were also obtained after four coats for *R* = 3 and five coats for *R* = 2. In this case, the apparition of cracks during the final annealing at 1000 °C may be due to the increase of the remaining content of organic compounds in the multilayers.

4. Discussion

The microstructure of a film can be modified through the nucleation and the dimensionality of crystal growth during its synthesis. Thus, it depends on the heat treatment, the organic compounds content and the La/Ni molar ratio. The driving force for grain growth is the reduction of grain boundary energy that results from the reduction of the total grain boundary area [16].

For high organic compounds content, the grains size distribution of C[(3,2)] films remains monomodal and their shape has no change with heating temperature. This characterizes a normal grain growth (3D crystal growth), leading to the formation of films randomly oriented.

For lower organic compound content, the coarse microstructure of C[(2,2)] films is predominantly obtained from abnormal grain growth (2D crystal growth). This mechanism occurs after a normal grain growth. A change in the shape of the grains size distribution is observed when the films are heated at 1000 °C. A bimodal distribution is observed, due to a faster growth of some grains at the expense of other ones. This indicates that the abnormal growth is not complete at this stage.

In our synthesis conditions, the occurrence of either normal or abnormal grain growth is mostly explained by a difference in the crystallization temperature. Indeed, this temperature governs the rates of nucleation and growth processes [16]. Previous thermal analyses showed that the crystallization started during the burnout of the organic compound around 430 °C. The germs size is lower than 10 nm whatever the *R* ratio used [17]. It was also shown that the higher the *R* ratio, the higher the heat released, the faster the kinetic reactions rates. Accordingly, in situ X-ray diffraction analyses showed that the crystallization temperature is lower for *R* = 3 compared to that for *R* = 2. Thus, the nucleation process is favored for high *R* ratios, leading to the formation of

a majority of smaller grains in the film volume. The mean grain size remains lower than the film thickness in this case, even at 1000 °C. For $R = 2$, the growth process is preferred, and the grains size reaches more quickly the films thickness, leading to the abnormal grain growth.

Control of the sol synthesis parameters allows the synthesis of $La_{2-x}NiO_{4+\delta}$ ($x \geq 0$) thin films with specific microstructures in terms of the shape of the grains, the grains size distribution, the material texture, the grains size and the porosity. Accordingly, drastic changes in both the electrical and the electrochemical properties of these electrodes may be attempted and some of the results are presented in a forthcoming paper [10]. Indeed, the interconnecting pore-solid architecture and the 3D network of bonded nanoscale particles of $La_2NiO_{4+\delta}$ electrodes prepared with $R = 3$ should facilitate both the ionic and the electronic conductivities and minimize the solid-state transport distances of ion-insertion reactions. This leads to low cathodic polarization resistances, in agreement with our electrochemical test results (0.12 Ω cm^2 measured for an electrode of 350 nm at 700 °C) [10].

At the contrary, the coarse microstructure of $La_2NiO_{4+\delta}$ films for $R = 2$ is attempted to reduce the mixed conduction and the specific area because of the pore-solid architecture, the large pores size (100 nm–1 μm) and the shape of the grain. Indeed, their polarization resistance is about four times higher than the one obtained for electrodes prepared with $R = 3$ (0.47 Ω cm^2 measured for an electrode of 350 nm at 700 °C).

The preparation of porosity and composition graded electrodes allows the synthesis of denser electrodes with a homogeneous pore-solid architecture, small pores and a 3D network of bonded particles. This should promote efficient electronic and ionic conductivities and increase the oxygen surface exchange. Indeed, the measured polarization resistances of these materials are among the lower ones obtained, despite the fact that the composition and porosity grades have not yet been optimized. Indeed, the as-measured polarization resistances are lower than the one measured by other authors, which reported polarization resistance of about 30 Ω cm^2 at 700 °C for thick electrode (15 μm) [5]. Moreover, further performance gains are to be expected with optimization of the cathode current collectors.

5. Conclusions

Homogeneous, crack-free, porous $La_{2-x}NiO_{4+\delta}$ ($x \geq 0$) films have been prepared onto YSZ substrates using a polymeric precursor synthesized via a chemically modified Pechini process. In order to synthesize composition and porosity graded cathodic interlayers, several coats have been deposited using either the same polymeric precursor or sols with different compositions in terms of organics concentration and ratio of lanthanum to nickel. This leads to very large differences in the pore-solid architecture, the particle size and the grain shape. Low organic concentration allows the synthesis of cathodic interlayer with fine microstructure and spherical grain of about 50 nm, while coarse microstructure with platelets is obtained for higher concentration. These microstructures are due to either a normal grain growth or an abnormal one, mainly influenced by the organics concentration. The number of coats and the withdrawal speed influence the films thickness and multilayers with a maximal thickness of 450 nm are obtained. Controlled both film microstructure and composition can be easily achieved by changing processing parameters. The present study underscores the importance of derived sol–gel method for synthesizing controlled cathodic interlayers (composition and porosity).

References

[1] J.J. Butte, in: S.C. Singhal, M. Dokiya (Eds.), Solid Oxide Fuel Cells VIII, Electrochem. Society, Pennington, NJ, 2003, pp. 16–30.
[2] Ulf. Bossel, in: S.C. Singhal, M. Dokiya (Eds.), Solid Oxide Fuel Cells VIII, Electrochem. Society, Pennington, NJ, 2003, pp. 127–134.
[3] J. Liu, S.A. Barnett, Solid State Ionics 158 (2003) 11–16.
[4] E.P. Murray, T. Tsai, S.A. Barnett, Solid State Ionics 110 (1998) 235–243.
[5] E. Boehm, Ph.D. Thesis, Bordeaux University, 2002.
[6] M. Kleitz, F. Petitbon, Solid State Ionics 92 (1996) 65–74.
[7] R.E. Williford, P. Singh, J. Power Sources 128 (2004) 45–53.
[8] D. Herbstritt, A. Weber, E. Ivers-Tiffée, J. Eur. Ceram. Soc. 21 (2001) 1813–1816.
[9] E. Ivers-Tiffée, A. Weber, D. Herbstritt, J. Eur. Ceram. Soc. 21 (2001) 1805–1811.
[10] M.-L. Fontaine, C. Laberty-Robert, S.A. Barnett, F. Ansart, P. Tailhades, submitted for publication.
[11] Pechini Patent, 3,330,697, July 11 (1967).
[12] M.-L. Fontaine, C. Laberty-Robert, F. Ansart, P. Tailhades, J. Solid State Chem. 177 (2004) 1471–1479.
[13] M.-L. Fontaine, Ph.D. Thesis, Toulouse University, 2004.
[14] M.-L. Fontaine, C. Laberty-Robert, F. Ansart, P. Tailhades, Ceram. Int. 30 (2004) 2087–2098.
[15] M. Gaudon, Ph.D. Thesis, 2002.
[16] H.P. Longworth, C.V. Thompson, J. Appl. Phys. 69 (1991) 3929–3935.
[17] C. Laberty-Robert, M.-L. Fontaine, T. Mounis, B. Mierzwa, J. Pielaszeck, Solid State Ionics 176 (2005) 1213–1223.